Mon. Not. R. Astron. Soc. **347,** L57–L60 (2004)

L_X–SFR relation in star-forming galaxies

M. Gilfanov,[1,2]★ H.-J. Grimm[1] and R. Sunyaev[1,2]
[1] *Max-Planck-Institut für Astrophysik, 85741 Garching bei München, Germany*
[2] *Space Research Institute, 117997, 84/32 Profsoyuznaya Str, Moscow, Russia*

Accepted 2003 November 20. Received 2003 November 18; in original form 2003 January 16

ABSTRACT

We compare the results of Grimm, Gilfanov & Sunyaev and Ranalli, Comastri & Seti on the L_X–SFR (X-ray luminosity–star formation rate) relation in normal galaxies. Based on the L_X–stellar mass dependence for low-mass X-ray binaries (LMXBs), we show that low-SFR ($\lesssim$1 $M_\odot$ yr^{-1}) galaxies in the Ranalli et al. sample are contaminated by the X-ray emission from LMXBs, unrelated to the current star formation activity.

However, the most important conclusion from our comparison is that, after the data are corrected for the 'LMXB contamination', the two data sets become consistent with each other, despite differences in their content, variability effects, adopted source distances, X-ray fluxes and SFR determinations, and also in the cosmological parameters used in interpreting the *Hubble Deep Field* North (HDF-N) data. They also agree well, both in the low- and high-SFR regimes, with the predicted L_X–SFR dependence derived from the parameters of the 'universal' high-mass X-ray binary (HMXB) luminosity function. This encouraging result emphasizes the potential of the X-ray luminosity as an independent SFR indicator for normal galaxies.

Key words: galaxies: starburst – X-rays: binaries – X-rays: galaxies.

1 INTRODUCTION

Based on *Chandra* observations of nearby star-forming galaxies and studies of high-mass X-ray binary (HMXB) population in the Milky Way and the Small Magellanic Cloud (SMC), Grimm et al. (2003) proposed recently that HMXBs can be used as a star formation rate (SFR) indicator. They found that, in a broad range of star formation regimes and rates, the X-ray luminosity (L_X) distribution of HMXBs can be approximately described by a 'universal' luminosity function – a power law with a slope of ~1.6 and a cut-off at $\log(L_X) \sim 40.5$, the normalization of which is proportional to the SFR. As the 2–10 keV luminosity L_X of a normal galaxy with sufficiently high SFR/M_* ratio (where M_* is the total stellar mass) is dominated by the emission from HMXBs, the X-ray luminosity can be used as a SFR indicator for normal galaxies.

Although the normalization of the luminosity function and the number of sources are proportional to the SFR, the L_X–SFR dependence is non-linear in the low-SFR regime, becoming linear only at sufficiently high values of the SFR (thick solid line in Fig. 1). This non-linear behaviour at low SFR values is *not* related to intrinsic non-linear SFR-dependent effects in the population of the HMXB sources. Rather, it is caused by the fact that the quantity of interest is a sum of the luminosities of discrete sources – $L_{X,\rm tot} = \sum_k L_{X,k}$, with $L_{X,k}$ obeying a power-law luminosity distribution. The non-linear behaviour is caused by the properties of the $p(L_{X,\rm tot})$ probability distribution – namely, the difference between its expectation mean (average) and its mode (most probable value). This effect was discussed in Grimm et al. (2003) and Gilfanov (2004) and will be given a detailed treatment in Gilfanov, Grimm & Sunyaev (in preparation). The position of the break in the L_X–SFR relation is defined by the parameters of the luminosity function. For particular values of the slope and the cut-off luminosity found by Grimm et al. (2003), the boundary between the non-linear and linear regimes lies at SFR $\sim 4.5 M_\odot$ yr^{-1} or, equivalently, $L_X \sim 3 \times 10^{40}$ erg s^{-1}. *Chandra* and *ASCA* measurements of the total X-ray luminosity of a number of nearby star-forming galaxies were in good qualitative and quantitative agreement with the predicted L_X–SFR relation (Fig. 1, thick solid line and filled circles). Moreover, the distant star-forming galaxies, observed by *Chandra* in the *Hubble Deep Field* North (Brandt et al. 2001) at redshifts of $z \sim 0.2$–1.3, also obey the same relation. In the linear high-SFR regime, it is given by

$$\mathrm{SFR}[M_\odot\,\mathrm{yr}^{-1}] = \frac{L_{2-10\,\mathrm{keV}}}{6.7 \times 10^{39}\,\mathrm{erg\,s^{-1}}}, \quad (1)$$

where SFR is the formation rate of massive stars, $M > 5\ M_\odot$. Grimm et al. (2003) pointed out the importance of two contaminating factors, unrelated to the current star formation activity: (i) the emission of the central supermassive black hole, which even in the low luminosity active galactic nuclei (AGNs) can easily outshine X-ray binaries; and (ii) the contribution of the low-mass X-ray binaries (LMXBs), which might be especially important in the low-SFR regime.

★E-mail: gilfanov@MPA-Garching.MPG.DE

Ranalli et al. (2003) independently studied X-ray luminosity of normal galaxies using the *ASCA* and *BeppoSAX* archival data and *Chandra* observations of the HDF-N; they found a tight correlation between their X-ray, radio (1.4 GHz) and far-infrared (FIR) fluxes. They suggested that the 2–10 keV luminosity of normal galaxies can be used as an SFR indicator and derived the relation

$$\mathrm{SFR}[\mathrm{M}_\odot\ \mathrm{yr}^{-1}] = \frac{L_{2-10\,\mathrm{keV}}}{5\times10^{39}\ \mathrm{erg\ s^{-1}}}. \tag{2}$$

This formula agrees reasonably well with that obtained by Grimm et al. (2003) for the high-SFR regime [equation (1)]. However, Ranalli et al. (2003) noted that the L_X–SFR relation was linear in the entire range of the SFRs, including the low-SFR regime, in apparent contradiction to the results of Grimm et al. (2003).

In this Letter, we compare the Grimm et al. (2003) and Ranalli et al. (2003) samples of the galaxies. We demonstrate that the X-ray emission from the low-SFR galaxies in the Ranalli et al. (2003) sample is likely to be 'contaminated' by LMXBs, which are unrelated to current star formation activity. After the 'LMXB contamination' is accounted for, the two data sets agree qualitatively and quantitatively and are consistent with the L_X–SFR relation expected on the basis of the 'universal' HMXB luminosity function derived by Grimm et al. (2003).

2 THE SAMPLES

In the following, we denote Ranalli et al. (2003) and Grimm et al. (2003) samples as R and G, respectively. The data from both samples are plotted together in Fig. 1.

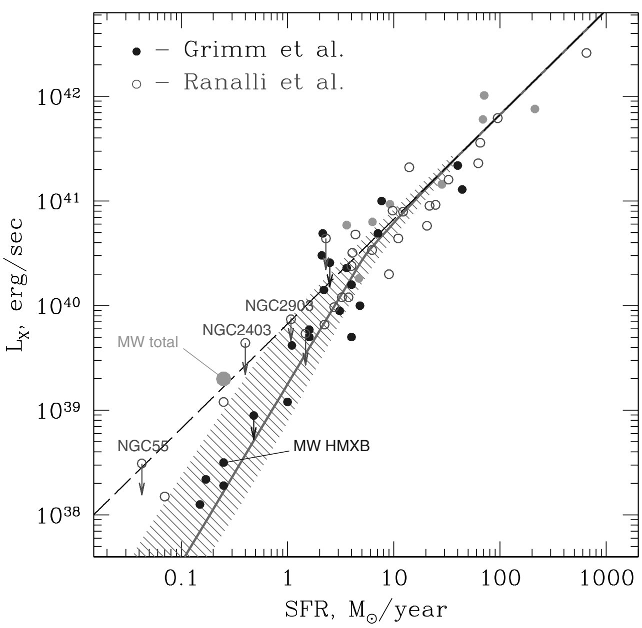

Figure 1. L_X–SFR relation. All points are from Ranalli et al. (2003) and Grimm et al. (2003) are plotted. The galaxies with the expected LMXB fraction exceeding 50 per cent are plotted as upper limits. The thick solid line shows the predicted relation between the most probable values of L_X and the SFR; the shaded area indicates its 67 per cent intrinsic spread. The straight dashed line shows the expectation mean for L_X, which would be obtained if X-ray luminosities of many galaxies with similar SFR were averaged. To demonstrate the importance of the LMXB contribution at low SFR/M_*, both HMXB and total luminosities are plotted for the Milky Way. This figure is available in colour in the online version of the journal on *Synergy*.

2.1 The local galaxies

The two samples, although differently constructed, overlap substantially, with nine galaxies (out of 23 in each sample) present in both. Sample R was derived using a more rigorously defined construction algorithm. In almost all cases, the authors adopted different distances and different values of the SFR. Grimm et al. (2003) derived SFR values by averaging the results of several independent estimators based on UV, FIR, H_α and radio flux measurements, whereas Ranalli et al. (2003) used radio flux measurements. The X-ray fluxes were obtained from different observations, sometimes by different instruments and are obviously affected by variability of the X-ray emission from the galaxies. For some of the galaxies, the X-ray luminosity was calculated by Grimm et al. (2003) as a direct sum of the luminosities of compact sources detected by *Chandra*.

Fig. 2 compares positions of the galaxies present in the both samples in the L_X–SFR plane. Note that the difference in the adopted distances does not have an effect at high values of SFR where the L_X–SFR relation is linear, but it might destroy the correlation in the non-linear low-SFR regime.

2.2 *Hubble Deep Field* North

Both Grimm et al. (2003) and Ranalli et al. (2003) used similar selection criteria. Each sample contains seven sources, of which six are present in both samples. Sources #185 and #148 (according to table 2 in Brandt et al. 2001) are absent from the R and G samples, respectively. The latter was excluded from sample G because no 1.4-GHz flux was detected, with the upper limit of 23 μJy (Richards et al. 1998). The main difference lies in computing the X-ray fluxes and luminosities. Grimm et al. (2003) used 2–8 keV fluxes from the *Chandra* catalogue and *K*-corrected them to a 2–10 keV

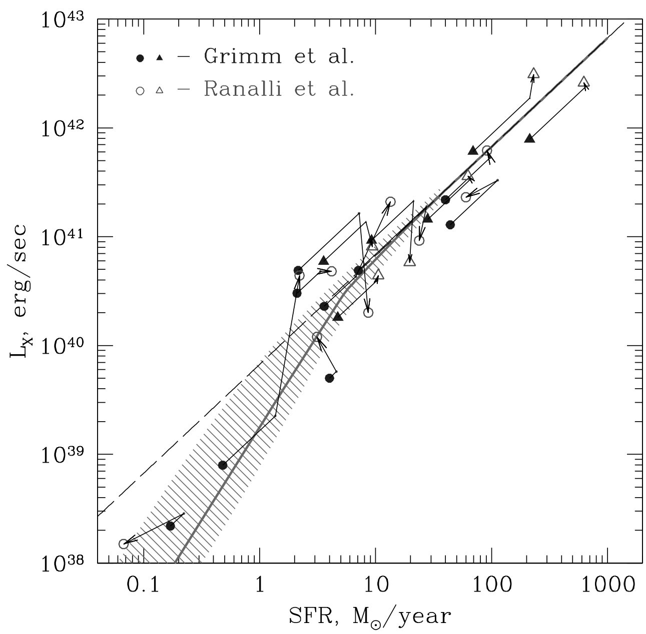

Figure 2. Comparison of the data for local (circles) and HDF-N (triangles) galaxies present both in Grimm et al. (2003) and Ranalli et al. (2003) samples. For each galaxy, its positions in two samples are connected by a broken line, with the arrow directed from G to R. The first segment of each broken line shows the effect of the difference in the source distance or cosmological parameters; the second segment shows the cumulative effect of other factors, such as variability and difference in the SFR values. This figure is available in colour in the online version of the journal on *Synergy*.

rest-frame luminosity using the spectral indexes from Brandt et al. (2001). Ranalli et al. (2003) derived the X-ray count rates in two redshift-corrected energy bands and based their final *K*-correction on the recomputed spectral indexes. The following cosmological parameters were used: $H_0 = 50$ km s^{-1} Mpc^{-1} and $q_0 = 0.1$ (sample R); $H_0 = 70$ km s^{-1} Mpc^{-1}, $q_0 = 0.5$ and $\Lambda = 0$ (sample G). The positions of the data points in the L_X–SFR plane are compared in Fig. 2.

3 LMXB CONTRIBUTION

Due to the long evolutionary time-scale, the population of LMXBs is unrelated to the current star formation activity. Rather, it is proportional to the stellar mass of the host galaxy (Gilfanov 2004). Hence, the X-ray emission from LMXBs can contaminate the L_X–SFR relation, as exemplified by the Milky Way, in which the LMXB contribution exceeds ≈90 per cent (fig. 1, Grimm, Gilfanov & Sunyaev 2002). Although LMXB and HMXB sources cannot be easily separated based on the X-ray data, and although optical identifications are (potentially) available only for the most nearby galaxies, the number and combined luminosity of LMXBs can be predicted sufficiently accurately based on the stellar mass of the host galaxy (Gilfanov 2004). Thus, relative contributions of LMXB and HMXB sources to the X-ray luminosity of the galaxy are defined by its position on the SFR–M_* plane (Fig. 3).

Stellar masses of the galaxies were calculated using *K*-band magnitudes from the Two-Micron All Sky Survey (2MASS) Large Galaxy Atlas (Jarrett, Chester & Cutri 2000) with the colour-based correction to the mass-to-light ratio (Bell & de Jong 2001). The mass of the Milky Way was calculated using its *K*-band luminosity obtained by Malhotra et al. (1996) from 3D modelling of the DIRBE data, and assuming the same mass-to-light ratio as in M31. The stellar masses of the Large Magellanic Cloud (LMC) and the SMC were estimated from their dynamical masses (Grimm et al. 2003), assuming $M_{\rm dyn}/M_* = 5$. The distances for the galaxies from sample G are the same as in Grimm et al. (2003). We re-examined the distance to low-SFR galaxies. For NGC 55 (1.6 Mpc) and M101 (7.2 Mpc), we adopted values from Puche, Carignan & Wainscoat (1991) and Jurcevic, Pierce & Jacoby (2000). The distances to NGC 2403 (3.7 Mpc), NGC 2903 (9.5 Mpc), NGC 4449 (3.8 Mpc) and NGC 4654 (17.6 Mpc) were estimated from the IR Tully–Fisher relation (Aaronson et al. 1982) using data from Tormen & Burstein (1995) and calibration from Sakai et al. (2000). The distances to other galaxies from the R sample are the same as in Ranalli et al. (2003).

The galaxies from the R and G samples are plotted in the SFR–M_* plane in Fig. 3, along with the contours of constant $L_{\rm HMXB}$:$L_{\rm LMXB}$ ratio. The luminosities of LMXB and HMXB sources were estimated from their respective average luminosity functions obtained by Grimm et al. (2003) and Gilfanov (2004). In estimating the LMXB luminosity, we used average normalization for late-type galaxies. Although linear relations hold in the limit of large number of sources ($L_{\rm LMXB} \propto M_*$ and $L_{\rm HMXB} \propto$ SFR), the contours are not straight lines at $M_* \lesssim 2 \times 10^{10}$ M$_\odot$ and SFR $\lesssim 4$ M$_\odot$ yr^{-1} due to effects of statistics (Gilfanov, Grimm & Sunyaev, in preparation).

As expected, the 'LMXB contamination' plays a role mostly at low SFR values and becomes unimportant at high SFR values. In all but one galaxy from sample R having SFR $\lesssim 1$ M$_\odot$ yr^{-1}, the expected contribution of LMXBs exceeds ∼50 per cent. These galaxies

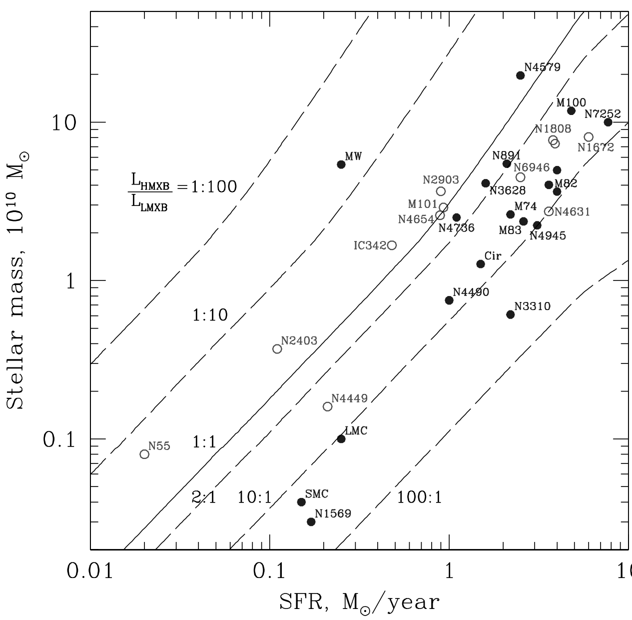

Figure 3. Location of galaxies from R (open circles) and G (filled circles) samples on the SFR–M_* plane. The dashed lines correspond to constant ratio of the the most probable values of HMXB and LMXB luminosities estimated from respective average luminosity functions, accounting for non-linear effects of statistics. For the points above the solid line, the LMXB contribution exceeds 50 per cent. This figure is available in colour in the online version of the journal on *Synergy*.

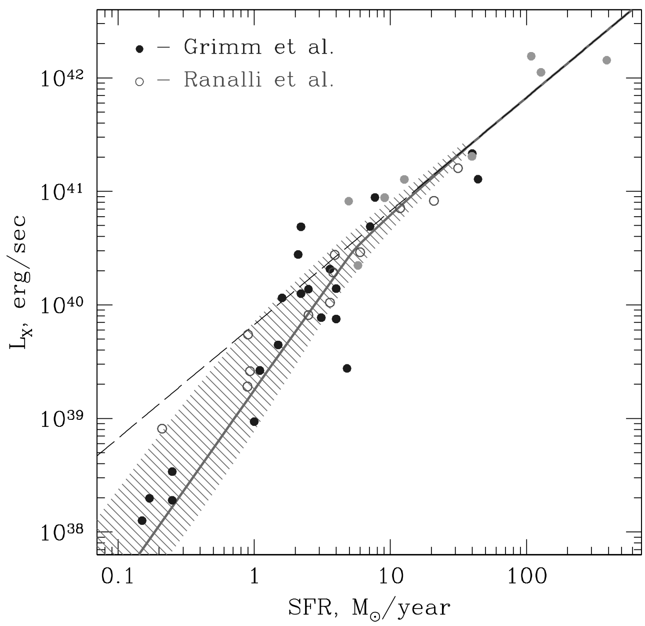

Figure 4. L_X–SFR relation. The data used is the combined data from Ranalli et al. (2003) and Grimm et al. (2003), with duplications excluded. The L_X values for nearby galaxies were corrected for the LMXB contribution estimated from the stellar mass. Three galaxies with more than 50 per cent LMXB contribution and small stellar mass, $M_* < 2 \times 10^{10}$ M$_\odot$, for which large intrinsic dispersion of the $L_X - M_*$ relation precludes accurate estimate of the LMXB luminosity are not plotted. The luminosities for the HDF-N and Lynx field galaxies were computed for $H_0 = 70$ km s^{-1} Mpc^{-1}, $\Omega_m = 0.3$, $\Lambda = 0.7$. The solid and dashed lines and the shaded area are the same as in Fig. 1. This figure is available in colour in the online version of the journal on *Synergy*.

are shown in Fig. 1 as upper limits. For two galaxies (NGC 55 and NGC 2403) mostly deviating from the common trend in Fig. 1, the expected LMXB contribution exceeds ~70 per cent.

4 COMBINED SAMPLE AND PREDICTED L_X–SFR RELATION

Fig. 4 shows all data from samples G and R, excluding duplications. The tightness of the L_X–M_* relation at large M_* (fig. 14 in Gilfanov 2004) allows one to correct observed luminosities approximately for the LMXB contribution. This correction was applied for all galaxies, except for those with $M_* < 2 \times 10^{10}$ M$_\odot$ and $L_{\rm HMXB} : L_{\rm LMXB} < 1$. These exceptions (NGC 55, NGC 2403 and IC 342) are not plotted in Fig. 4.

The solid curve in Fig. 4 shows the predicted L_X–SFR relation, calculated using the parameters of the 'universal' HMXB luminosity function derived by Grimm et al. (2003) from analysis of five nearby star-forming galaxies with best known luminosity functions. It corresponds to the mode of the probability distribution – the *most likely* value of the X-ray luminosity of a randomly chosen galaxy. The dashed line, on the contrary, shows the expectation mean – the value, that would result from *averaging* of the X-ray luminosities of many galaxies having similar SFR values. Due to the properties of the probability distribution of the total luminosity of a population of discrete sources, $L_{\rm X,tot} = \sum_k L_{{\rm X},k}$, these two quantities are not identical in the low-SFR limit when the number of sources is small.

Due to skewness of the probability distribution $p(L_{\rm X,tot})$ (fig. 2 in Gilfanov 2004), large and asymmetric dispersion around the solid curve in Fig. 4 is expected in the non-linear low-SFR regime. The probability of finding a galaxy below the curve is ≈12–16 per cent at SFR = 0.2–1.5 M$_\odot$ yr^{-1} and increases to ≈30 per cent at SFR = 4–5 M$_\odot$ yr^{-1}, near the break of the L_X–SFR relation. Of course, in the linear regime (SFR $\gtrsim$ 10 M$_\odot$ yr^{-1}), it asymptotically approaches ~50 per cent, as expected. This asymmetry is already seen from the distribution of the points in Fig. 4 – at low SFR values, there are more points above the solid curve than below. Moreover, the low-probability high-luminosity tail of the $p(L_{\rm X,tot})$ distribution will lead to the appearance of outlier galaxies with significantly larger than expected values of the total luminosity. Such galaxies will inevitably appear as the plot is populated with more objects. Non-Gaussianity of the $p(L_{\rm X,tot})$ distribution makes least-squares and χ^2 fitting techniques inadequate for analysis of the L_X–SFR relation in the low-SFR regime.

5 CONCLUSION

We compared results of Grimm et al. (2003) and Ranalli et al. (2003) on the relation between the X-ray luminosity and the SFR in normal galaxies (Figs 1 and 2).

Addressing the discrepancy in the low-SFR regime, we note that six out of seven galaxies from Ranalli et al. (2003), having SFR $\lesssim$ 1 M$_\odot$ yr^{-1}, are likely to be contaminated by the X-ray emission from LMXBs, having no relation to the current star formation activity. Furthermore, at $M_* \lesssim 10^{10}$ M$_\odot$ and SFR $\lesssim$ 1 M$_\odot$ yr^{-1}, the expected luminosity of X-ray binaries does not exceed $\lesssim 10^{39}$ erg s^{-1}. This is comparable or smaller than that of low-luminosity AGNs often found by *Chandra* in otherwise apparently normal galaxies. The AGN contribution can not be identified and separated, unless high angular resolution imaging data are available. Secondly, the probability distribution of the total luminosity of a population of discrete sources, $L_{\rm X,tot} = \sum_k L_{{\rm X},k}$, is significantly non-Gaussian for low values of $L_{\rm X,tot}$. This should not be ignored when analysing and interpreting the L_X–SFR relation in the low-SFR regime.

The most important conclusion is, however, that after the potentially 'LMXB contaminated' galaxies are excluded, the two data sets *become consistent* with each other, despite differences in their content, variability effects, adopted source distances, X-ray fluxes and SFR determinations, and also in the cosmological parameters used in interpreting the HDF-N data. The ~30 per cent difference in the calibration of the L_X–SFR relation is insignificant considering the number and amplitude of the uncertainties involved. They also agree well, both in the low- and high-SFR regimes, with the predicted L_X–SFR dependence derived from the parameters of the 'universal' HMXB luminosity function (Fig. 4). This is an encouraging result emphasizing the potential of the X-ray luminosity as an independent SFR indicator.

ACKNOWLEDGMENTS

We are grateful to the referee, Dr Pranab Ghosh, for critical and stimulating comments on the original manuscript which helped to improve the paper.

REFERENCES

Aaronson M. et al., 1982, ApJS, 50, 241
Bell E., de Jong R., 2001, ApJ, 550, 212
Brandt W. N. et al., 2001, AJ, 122, 2810
Gilfanov M., 2004, MNRAS, in press (astro-ph/0309454)
Grimm H.-J., Gilfanov M., Sunyaev R., 2002, A&A, 391, 923
Grimm H.-J., Gilfanov M., Sunyaev R., 2003, MNRAS, 339, 793
Jarrett T. H., Chester T., Cutri R., 2003, AJ, 125, 525
Jurcevic J. S., Pierce M. J., Jacoby G. H., 2000, MNRAS, 313, 868
Malhotra S. et al., 1996, ApJ, 473, 687
Puche D., Carignan C., Wainscoat R., 1991, AJ, 101, 447
Ranalli P., Comastri A., Seti G., 2003, A&A, 399, 39
Richards E. A. et al., 1998, AJ, 116, 1039
Sakai S. et al., 2000, ApJ, 529, 698
Tormen G., Burstein D., 1995, ApJS, 96, 123